

# Fabrication and properties of $\text{KMnO}_4$ -treated functionalized biaxially oriented polypropylene (BOPP) films coated with a hybrid material

Jing Wang · Yaofeng Zhu · Yaqin Fu

Received: 6 November 2013 / Accepted: 7 April 2014 / Published online: 16 April 2014  
© Springer Science+Business Media New York 2014

**Abstract**  $\text{KMnO}_4$ -treated functionalized biaxially oriented polypropylene (BOPP) films coated with a hybrid material were synthesized, and the abrasion resistance properties of the resultant films were examined. The presence of functional groups was confirmed using Fourier-transform infrared spectroscopy, transmittance measurements were performed using an ultraviolet–visible spectrophotometer, and the intensities of the films were measured using a universal testing machine. The abrasion resistance and roughness of the composite films were significantly affected by modification of the BOPP film. The transmittance of the modified films obviously improved with the addition of  $\text{Al}_2\text{O}_3$  sol, and the mechanical properties of the treated films were improved by the coatings. The abrasion resistance of one of the functionalized films (sample S159) increased by 79.5 % compared with that of the original film.

**Keywords** Abrasion resistance · Biaxially oriented polypropylene · Surface modification ·  $\text{KMnO}_4$

## 1 Introduction

Biaxially oriented polypropylene (BOPP) films are important commercial polyolefin films widely used in food packaging, as a protective coating of other films, and printing [1–4]. However, the relatively low adhesion and

scratch resistance of BOPP films restrain their wider application [5, 6]. Application of sol–gel coatings is the most commonly employed method for protecting BOPP films from direct contact with scratching particles. However, BOPP films exhibit very low surface tension, especially in the polar regions of the polymers; this low surface tension leads to incomplete wettability, which causes low interfacial interactions between the highly crosslinked coating and the polypropylene films. Thus, to improve the application prospects of BOPP films, surface modification techniques must be introduced.

The most commonly used surface treatment techniques for BOPP films include plasma treatment [7, 8], ion beam treatment [9], corona discharge [10], surface grafting [11], and chemical oxidation [12, 13]. Favaro et al. [14] demonstrated that the surface wettability of polypropylene films can be significantly improved by treatment with  $\text{KMnO}_4$  solution. In their study, the adhesion of  $\text{KMnO}_4$ -treated PP films improved, but the treated films were washed with HCl solution, which is not eco-friendly and could be harmful to researchers and end-users. Jeon et al. [15] prepared hard coating films based on organosilane-modified boehmite nanoparticles under UV/thermal dual curing. Wan et al. [16] and Lioni [17] synthesized hybrid materials using a sol–gel technique with the addition of water to successfully improve the abrasion resistance of the substrate. However, studies on the preparation of sol–gel solutions in the absence of water are limited [18]. Wang et al. [19] synthesized hybrid materials using a sol–gel technique without the addition of water; the resulting material had a low reaction rate, resulted in a more stable and easy-to-store sol system, and successfully improved the abrasion resistance of BOPP films. However, curing conditions were fairly rigorous at  $-55\text{ }^\circ\text{C}$  and 0.01 MPa and thus impractical for industrial applications.

J. Wang · Y. Zhu · Y. Fu (✉)  
The Key Laboratory of Advanced Textile Materials and  
Manufacturing Technology Ministry of Education, Zhejiang Sci-  
Tech University, Hangzhou 310018, Zhejiang, China  
e-mail: fyq01@zstu.edu.cn

In the current study,  $\text{KMnO}_4$  solution was used to modify the surface of BOPP films to improve their adhesion, and oxalic acid solution, which is more eco-friendly than  $\text{HCl}$ , was used to wash the treated films. A sol–gel method in which the sol is synthesized without the addition of deionized water was used to prepare uniformly dispersed nanoparticles, and  $\text{Al}_2\text{O}_3$  sol was added to the  $\text{SiO}_2$  sol to maintain the high transmittance of treated BOPP films. The BOPP films were then coated with the hybrid material using a dip-coating technique.

## 2 Experimental

### 2.1 Materials

BOPP films (thickness = 47  $\mu\text{m}$ ) were supplied by Zhejiang Kelly Packaging Materials Company (China).  $\text{KMnO}_4$ , 98 % (w/v)  $\text{H}_2\text{SO}_4$  solution, tetraethoxysilane (TEOS), *p*-toluene sulfonic acid (PTSA), absolute ethanol (99.7 wt%), oxalic acid, aluminum tri-sec-butoxide (ASB), and 3-triethoxysilylpropylamine (KH550) were provided by Hangzhou Mike Chemical Instrument (China). All chemicals were used without further purification.

### 2.2 Surface modification of BOPP films

The BOPP films were washed with deionized water and dried in a baking oven prior to modification. The films were oxidized in 0.3/0.1 M  $\text{KMnO}_4/\text{H}_2\text{SO}_4$  solution at 60 °C for 6 h, yielding films with good adhesion properties [14]. Afterward, the BOPP films were washed with oxalic acid solution to remove any oxidation residue from their surface.

### 2.3 Preparation of surface modifier

A total of 30.00 g of TEOS, 0.30 g of PTSA, and 200 mL of ethanol were added to a small reaction vessel at room temperature under stirring for 2 h. The obtained homogeneous mixture was marked solution A. Exactly 6.00 g of KH550 and 200 mL of ethanol were added to another small reaction vessel at room temperature under stirring for 2 h, and the resulting mixture was marked solution B. Solution B was added to solution A using the titrimetric method under stirring for 2 h. The resulting Sol 1 was stored in a fresh vessel and isolated from air. In the same manner, a total of 10.00 g of ASB and 200 mL of ethanol were added to a small reaction vessel at room temperature under stirring for 2 h. The resulting solution was marked solution C. Exactly 0.10 g of PTSA and 200 mL of ethanol were added to a small reaction vessel at room temperature under stirring for 2 h. The resulting solution was marked solution D. Solution C was added to solution D using the titrimetric

**Table 1** Sol compositions obtained using different ratios of the raw materials

Formula	TEOS/ASB (g)	PSTA (g)	KH550 (g)	EtOH (mL)
1	15/0	0.15	3	200
2	15/1	0.16	3	240
3	15/3	0.18	3	320
4	15/9	0.24	3	560
5	0/15	0.15	0	600

method under stirring for 2 h, thereby forming Sol 5. Sol 1 was mixed with Sol 5 at varying ratios, as shown in Table 1, to form different sol solutions.

### 2.4 Coating and curing

BOPP films modified with the  $\text{KMnO}_4/\text{H}_2\text{SO}_4$  solution were dipped into the sol solutions for 10 min, and the films were collected at a rate of 2 mm/s. The coated films were aged at 25 °C in the air for 24 h and then dried at 100 °C for 0.5 h. In this study, six samples labeled S150u, S150, S151, S153, S159, and S015 were prepared to determine the effects of the nanocomposite coatings on the BOPP films. S150u refers to the pristine film without treatment with  $\text{KMnO}_4/\text{H}_2\text{SO}_4$  solution but coated with Sol 1. S150, S151, S153, S159, and S015 refer to the films treated with  $\text{KMnO}_4/\text{H}_2\text{SO}_4$  solution and coated with Sol 1, Sol 2, Sol 3, Sol 4, and Sol 5, respectively.

### 2.5 Characterization

Changes in the surface functional groups were recorded on a Fourier-transform infrared (FTIR) spectrometer (Nicolet 5700, Thermo Electron Scientific Instruments Corp, USA). The surface topography of the BOPP films was analyzed after the abrasion test using a field-emission scanning electron microscope (Ultra 55, Zeiss, Germany) at an operating voltage of 3 kV. Sol dispersion was examined using a transmission electron microscopy (TEM) system (JEM-2100F, JEOL, Japan) operated at 200 kV. Transmittance measurements were performed using an ultraviolet–visible spectrophotometer (TU-1901, Persee, China), and the measured wavelengths were range from 400 to 800 nm. The transmission values were averaged from 400 to 800 nm, and each sample was measured six times. The chemical binding of the coated films was investigated by X-ray photoelectron spectroscopy (K-Alpha, Thermo Fisher Scientific, USA). The instrument was equipped with a monochromatic  $\text{Al-K}\alpha$  X-ray source ( $h\nu = 1,468.6$  eV), and the XPS analysis chamber was evacuated to a pressure of  $2 \times 10^{-9}$  mbar or lower before collecting XPS spectra. Spectra was collected using an X-ray spot size of 400  $\mu\text{m}$

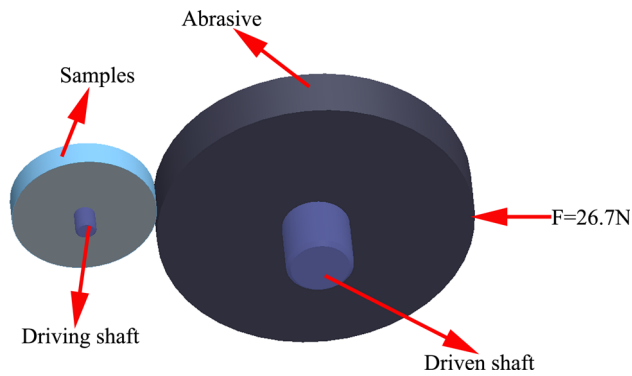


**Fig. 1** Schematic of the abrasion tester

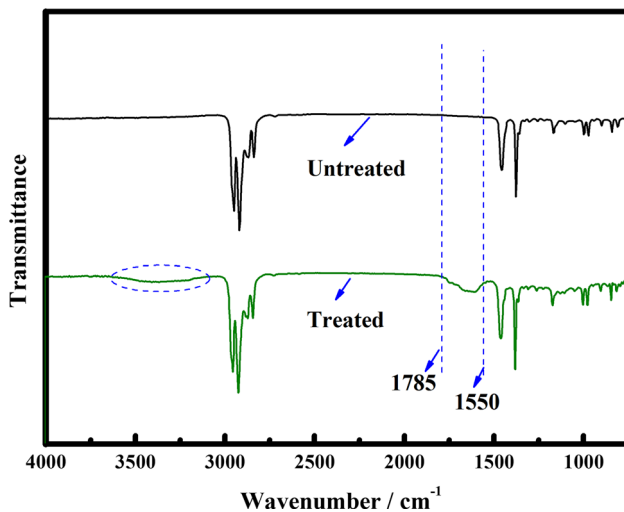


**Fig. 2** FTIR-ATR spectra of BOPP films with and without 0.3 M  $\text{KMnO}_4$  solution treatment

and pass energy of 100 eV, with 1 eV increments, at a  $90^\circ$  takeoff angle. The tensile property of the films was measured using a universal testing machine (INSTRON 3367,

USA), and ten samples with identical characteristics were tested. The abrasion resistance of the films was analyzed using an Akron abrasion tester (MH-74, China) (Fig. 1) at a loading of 26.7 N for 200 circles. Samples were cut into  $214 \text{ mm} \times 12.7 \text{ mm}$  sizes for abrasion testing. Mass loss ( $M_L$ ) was defined as:

$$M_L = \frac{M_0 - M_f}{M_0} \times 100 \%$$

where  $M_0$  is the weight of samples before the abrasion test and  $M_f$  is the weight of samples after the abrasion test.

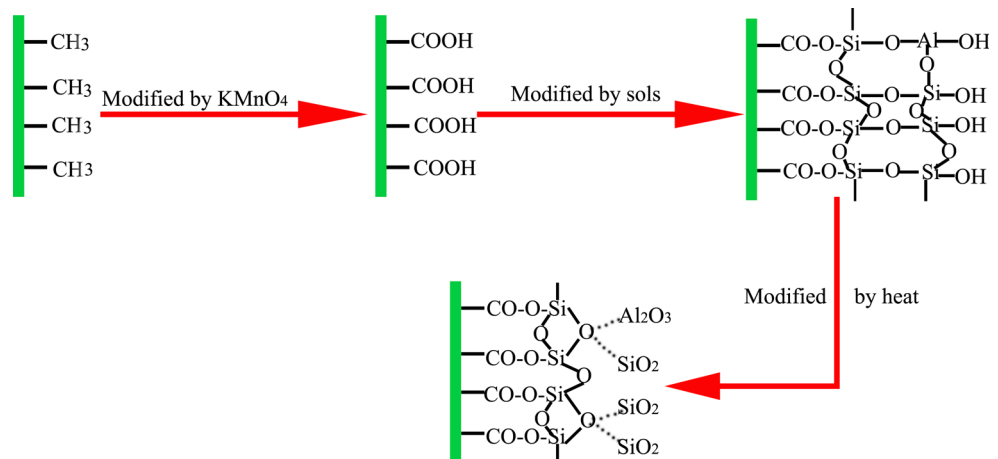
### 3 Results and discussion

#### 3.1 Effects of surface modification and mixed sol analyzed by FTIR

Figure 2 shows the FTIR spectra of raw BOPP films and modified BOPP films with  $\text{KMnO}_4$  solution. The main spectral changes found in the region between  $1,785$  and  $1,550 \text{ cm}^{-1}$  in the modified and untreated polymers are attributed to the different carbonyl groups that formed on the modified film surfaces. The mechanism diagram of preparation of BOPP composite films is shown in Fig. 3. In Fig. 2, the spectra of the treated BOPP films exhibit significant absorption bands at approximately  $1,785$  and  $1,550 \text{ cm}^{-1}$ , which correspond to  $-\text{C}=\text{O}$  and  $-\text{C}-\text{O}$  stretching vibrations, respectively. The treated films also show a broad band at around  $3,200 \text{ cm}^{-1}$ , which is attributed to  $\text{O}-\text{H}$  stretching vibrations. The spectra of the BOPP films indicate that surface modification using the  $\text{KMnO}_4$  solution can significantly promote the formation of oxygen-containing functional groups.

Figure 4 shows the FTIR spectra of the mixed sols. The absorption peak at  $951 \text{ cm}^{-1}$  attributed to  $\text{Si}-\text{OH}$  stretching vibrations shifted to  $905 \text{ cm}^{-1}$  upon addition of the  $\text{Al}_2\text{O}_3$  sol. When the  $\text{Al}_2\text{O}_3$  sol is added to the  $\text{SiO}_2$  sol, the

**Fig. 3** The mechanism diagram of preparation of BOPP composite films



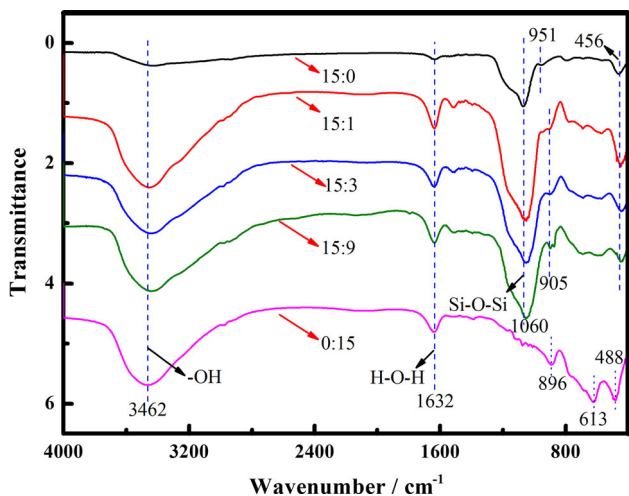


Fig. 4 FTIR spectra of various sols

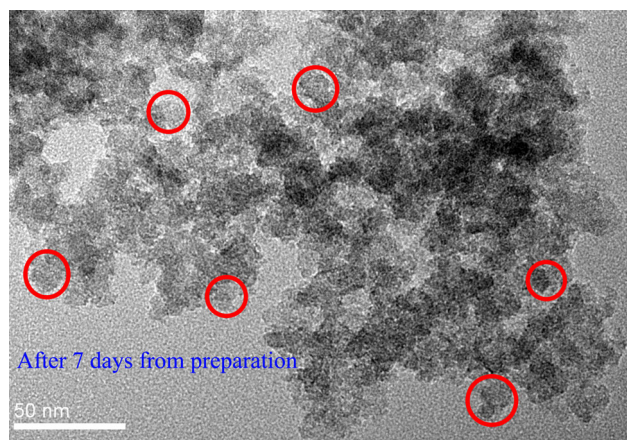


Fig. 5 TEM image of the sol (TEOS/ASB = 15:0) after 7 days from preparation

Si-OH groups are replaced by Si-O-Al; thus, the peak at 905 cm<sup>-1</sup> is attributed to Si-O-Al stretching vibrations. These findings confirm that the Si-O-Al group is formed in the mixed sol system.

### 3.2 Morphologies of the nanoparticles and sols

The morphology of the nanoparticles was investigated using TEM. Figure 5 shows that the average size of the nanoparticles is 20 nm. The formation of nanoparticles in the presence of water in air showed a low reaction rate and led to a more stable, transparent, and easy-to-store sol system compared with a water system. Figure 6 shows that the sols remain stable when isolated from air without addition of deionized water. The sols remained transparent even after aging for 30 days, which indicates that the sols prepared in this study may be conveniently stored and utilized in industrial applications.

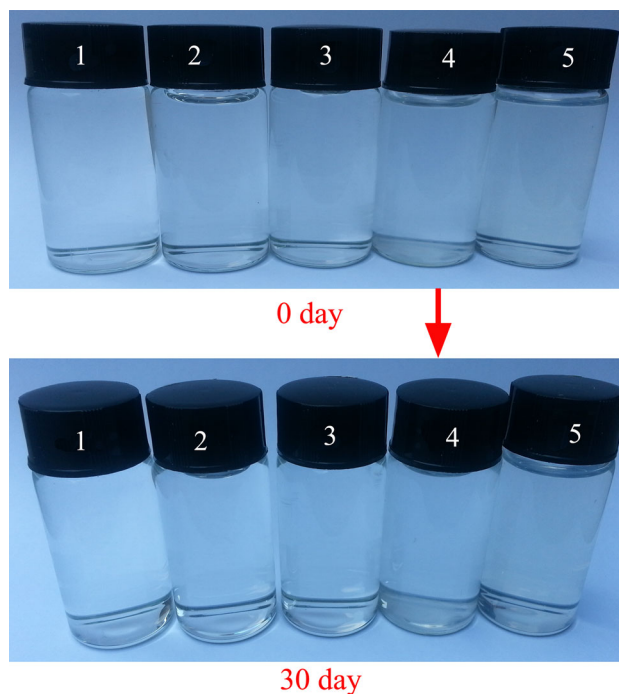


Fig. 6 Sol aging at different time points

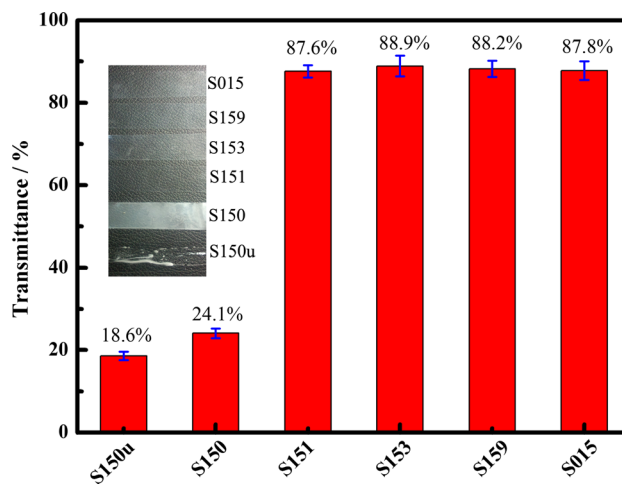
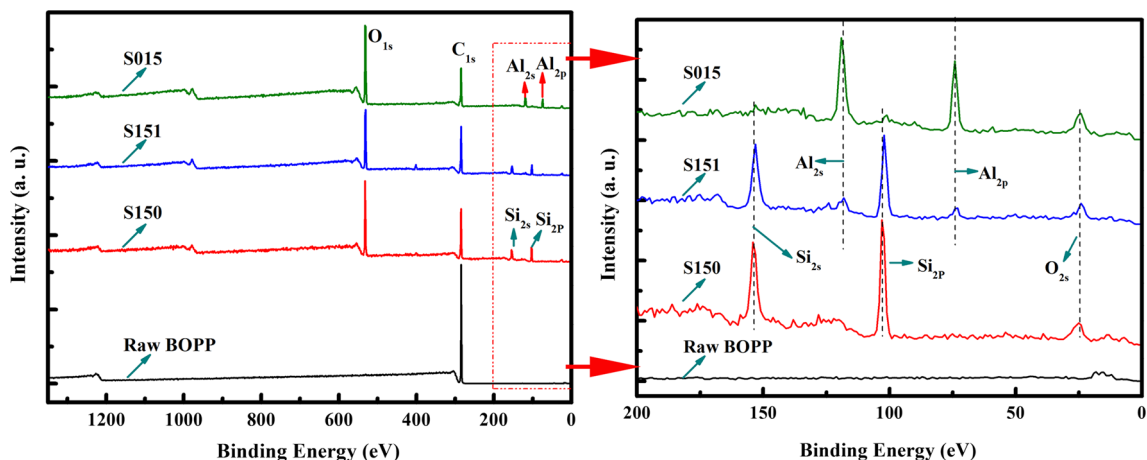


Fig. 7 Transmittance in the visible range of samples coated with various sols

### 3.3 Effect of surface modification on the transmittances of coated BOPP films

S150u, S150, S151, S153, S159, and S015 exhibited visible range (400–800 nm) transmittances of 18.6, 24.1, 87.6, 88.9, 88.2, and 87.8 %, respectively (Fig. 7). Compared with S150u, S150 exhibited considerably higher transmittance because surface modification can enhance interfacial interactions between the highly crosslinked coating and polypropylene films and smoothens the coating considerably.



**Fig. 8** XPS spectra of raw and various coated films

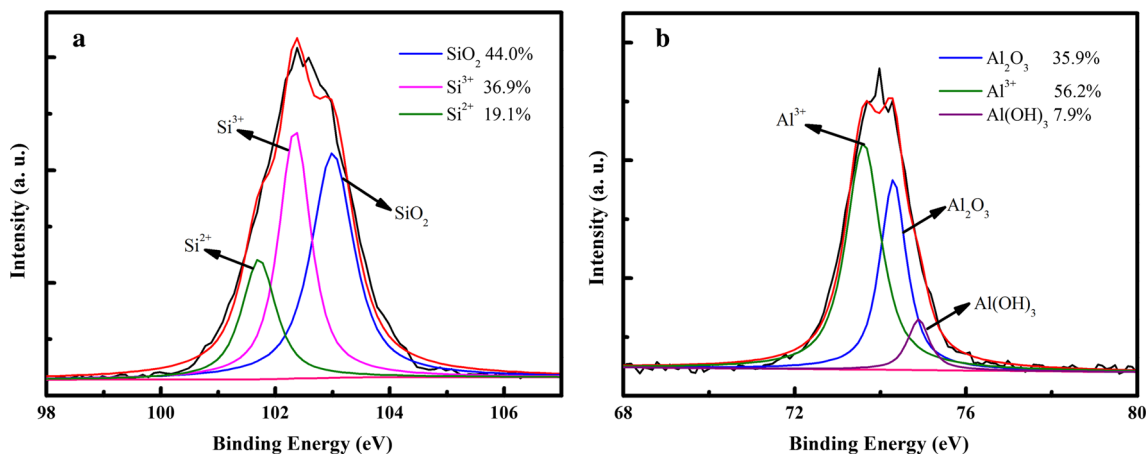


**Fig. 9** **a** Si<sub>2p</sub> spectra of sample S150 and **b** Al<sub>2p</sub> spectra of sample S015

S151, S153, S159, and S015, where were coated with the Al<sub>2</sub>O<sub>3</sub> sol, were all transparent, which suggests that coating with the Al<sub>2</sub>O<sub>3</sub> sol produces films with high transmittance.

### 3.4 XPS study of the coated films

Figure 8 compares the XPS spectra of the uncoated and coated films. According to the data in the NIST X-ray Photoelectron Spectroscopy database, the appearance of Al<sub>2s</sub> at 119.2 eV and Al<sub>2p</sub> at 74.3 eV confirms the formation of Al<sub>2</sub>O<sub>3</sub>. The formation of SiO<sub>2</sub> is also proven. All binding energies were referenced to the C<sub>1s</sub> hydrocarbon peak at 283 eV. The raw BOPP film is not oxidized by air, since O<sub>1s</sub> peaks were not observed. To analyze changes in the chemical composition of the BOPP film surface as well as their

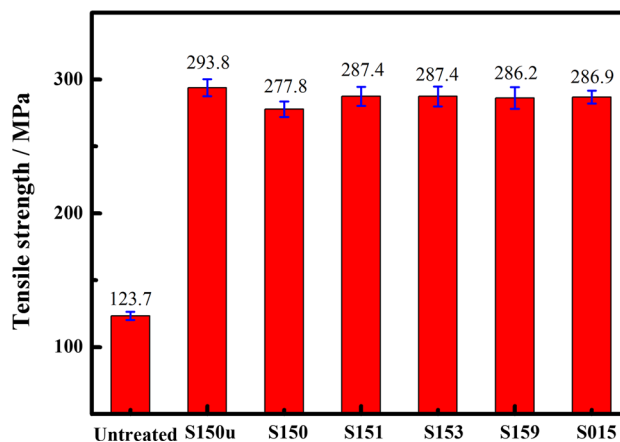


**Fig. 10** Tensile strength of the samples

chemical binding states, the spectra of Al2p and Si2p were investigated, as shown in Fig. 9. On the basis of the mechanism diagram of preparation of BOPP composite films (Fig. 3), the peaks were split to concrete compositions. The spectra obtained indicate that Al and Si elements in the films mainly exist as  $Al^{3+}$  and  $SiO_2$ , respectively. Various covalent bonds improved interfacial interactions between the highly crosslinked coating and the polypropylene films.

### 3.5 Effects of surface coating on the mechanical properties of the BOPP films

The samples were tested to study the effects of coating on their mechanical properties. The tensile strengths of the samples are shown in Fig. 10. The coating considerably

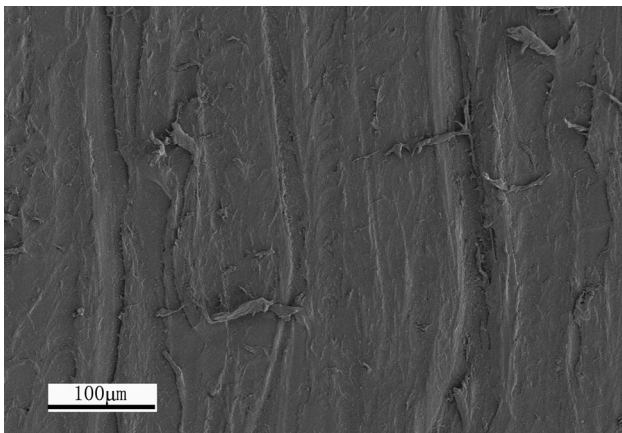


**Fig. 11** SEM image of the surface of the raw film after abrasion test

affected the mechanical properties of the BOPP films. Compared with the raw BOPP film, treated films exhibit significantly increased tensile strength. During the preparation of different sols, no water was added to the sol–gel systems. The precursors were hydrolyzed by air moisture in the process of gel, which effectively controls the rate of hydrolysis and results in finer and more uniform nanoparticles. Thus, sols can easily infiltrate the surface of the BOPP films and ultimately improve their mechanical properties. The tensile strength of S150 was slightly lower than that of S150u because surface modification can produce flatter and more uniform coatings without agglomeration.

### 3.6 Effect of surface coating on the abrasion resistance of BOPP films

The samples were subjected to abrasion treatment to study the effects of the coatings on the abrasion resistance of BOPP films. The surface morphologies of the BOPP films after the abrasion test are shown in Figs. 11 and 12. The raw film sample contained deep grooves, as shown in Fig. 11. Scratches on the surfaces of samples S150u and S150 can clearly be seen, but these scratches are shallower than those in the raw film sample. These results indicate that the abrasion resistance of the films is improved by the  $SiO_2$  sol coating and surface modification. Figure 12 further shows shallow grooves on the surfaces of S151, S153, S159, and S015, which indicate significant improvements in abrasion resistance compared with those of the raw film, S150u, and S150 samples. This result shows that addition of the  $Al_2O_3$  sol improves interfacial interactions between

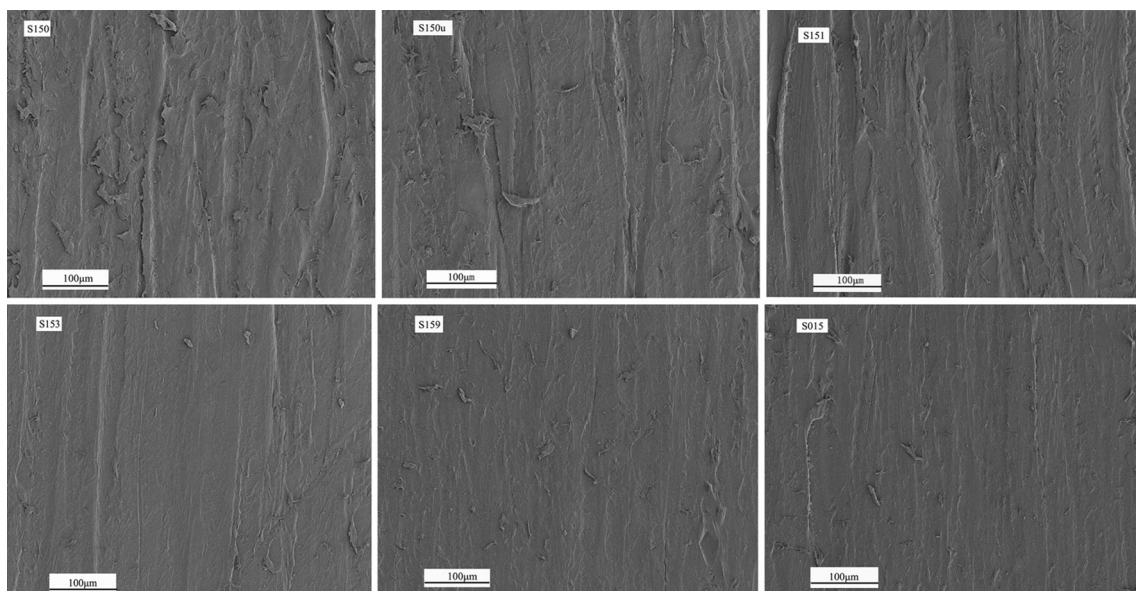


**Fig. 12** SEM image of the surfaces of the treated films after abrasion test

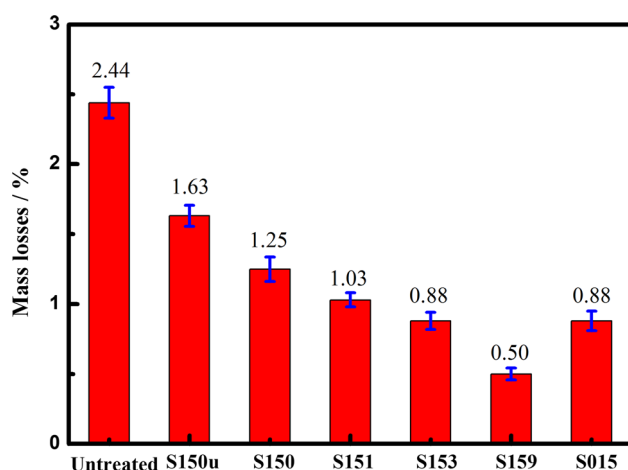


**Fig. 13** Mass losses of the samples after the abrasion test

the BOPP film and the coating, thereby resulting in higher abrasion resistance.

The MLs of the samples are shown in Fig. 13. The MLs of S150u, S150, S151, S153, S159, and S015 were 2.44, 1.63, 1.25, 1.03, 0.88, 0.50, and 0.88 %, respectively. These results suggest that surface modification of BOPP films through  $\text{KMnO}_4/\text{H}_2\text{SO}_4$  and coating treatment can significantly improve the abrasion resistance of the resultant films. The use of mixed sols obtained by addition of the  $\text{Al}_2\text{O}_3$  sol to the  $\text{SiO}_2$  sol can further improve the abrasion resistance of BOPP films. These findings were confirmed by SEM observations and are attributed to the strengthening effects of the nanoparticles on the film surfaces [20] as well as the presence of polar groups, both of which significantly improve the interfacial properties of the films [21]. In the current study, comparison of the results of the raw film sample with those of S159 showed that the abrasion resistance of the modified BOPP film increased by 79.5 %.

#### 4 Conclusion

Several surface modification conditions were applied to BOPP films. Modification with  $\text{KMnO}_4$  solution significantly increased interactions between the BOPPs films and the coating. The coating containing with  $\text{Al}_2\text{O}_3$  sol produces films with high transmittance. Uniformly dispersed nanoparticles were obtained by the sol–gel method, and the sols remained stable without the addition of deionized water. BOPP films exhibited high abrasion resistance after modification, and a maximum improvement of 79.5 % was observed.

**Acknowledgments** The authors gratefully acknowledge the Instrumental Analysis Center of Zhejiang Sci-Tech University for allowing the use of their characterization facilities. We also thank the technicians for their assistance in the analyses and for the technical discussions.

#### References

- Lin Y, Hiltner A, Baer E (2010) A new method for achieving nanoscale reinforcement of biaxially oriented polypropylene film. *Polymer* 51:4218–4224
- Kalapat N, Amornsakchai T (2012) Surface modification of biaxially oriented polypropylene (BOPP) film using acrylic acid-corona treatment: part I. Properties and characterization of treated film. *Surf Coat Technol* 27:594–601
- Pandiyaraj K-N, Selvarajan V, Deshmukh R-R, Gao C (2009) Modification of surface properties of polypropylene (PP) film using DC glow discharge air plasma. *Appl Surf Sci* 255:3965–3971
- Tamura S, Kuramoto I, Kanai T (2012) The effect of molecular structure of polypropylene on stretchability for biaxially oriented film. *Polym Eng Sci* 52:1383–1393
- Dasari A, Rohrmann J, Misra R-D-K (2002) Micro-and nanoscale evaluation of scratch damage in poly (propylene)s. *Macromol Mater Eng* 287:889–903
- Xiang C, Sue HJ, Chu J, Coleman B (2001) Scratch behavior and material property relationship in polymers. *J Polym Sci, Part B: Polym Phys* 39:47–59
- Xie J, Xin D, Cao H, Wang C, Zhao Y, Yao L, Ji F, Qiu Y (2011) Improving carbon fiber adhesion to polyimide with atmospheric pressure plasma treatment. *Surf Coat Technol* 206:191–201
- Vesel A, Mozetic M (2012) Surface modification and ageing of PMMA polymer by oxygen plasma treatment. *Vacuum* 86:634–637
- Hite D-A, Colombe Y, Wilson A-C, Brown K-R, Warring U, Jordens R, Jost J-D, McKay K-S, Pappas D-P, Leibfried D, Wineland D-J (2012) 100-fold reduction of electric-field noise in an ion trap cleaned with in situ argon-ion-beam bombardment. *Phys Rev Lett* 109:103001
- Bian X, Chen L, Yu D, Wang L, Guan Z (2012) Impact of surface roughness on corona discharge for 30-year operating conductors in 500-kV ac power transmission line. *IEEE Trans Power Deliver* 27:1693–1695
- Kyomoto M, Moro T, Takatori Y, Kawaguchi H, Nakamura K, Ishihara K (2010) Self-initiated surface grafting with poly (2-methacryloyloxyethyl phosphorylcholine) on poly (ether–etherketone). *Biomaterials* 31:1017–1024
- Li J, Wang M, Shen Y (2012) Chemical modification on top of nanotopography to enhance surface properties of PDMS. *Surf Coat Technol* 206:2161–2167
- Ji W-G, Hu J-M, Liu L, Zhang J, Cao C (2007) Improving the corrosion performance of epoxy coatings by chemical modification with silane monomers. *Surf Coat Technol* 201:4789–4795
- Fávaro S-L, Rubira A-F, Muniz E-C, Radovanovic E (2007) Surface modification of HDPE, PP, and PET films with  $\text{KMnO}_4/\text{HCl}$  solutions. *Polym Degrad Stab* 92:1219–1226
- Jeon S-J, Lee J-J, Kim W, Chang T, Koo S (2008) Hard coating films based on organosilane-modified boehmite nanoparticles under UV/thermal dual curing. *Thin Solid Films* 516:3904–3909
- Wan Y, Sun B, Liu W, Qi C (2012) Tribological performance of fatty acid modification of sol–gel  $\text{TiO}_2$  coating. *J Sol Gel Sci Technol* 61:558–564

17. Lioni K, Toury B, Boissière C, Benayoun S, Miele P (2013) Hybrid silica coatings on polycarbonate: enhanced properties. *J Sol Gel Sci Technol* 65:1–9
18. Xu L, Fu Y, Du M (2011) Investigation on structures and properties of shape memory polyurethane/silica nanocomposites. *Chin J Chem* 29:703–710
19. Wang J, Zhu Y, Fu Y (2013) Abrasion resistance of biaxially oriented polypropylene films coated with nanocomposite hard coatings. *Appl Surf Sci* 285P:697–701
20. Xu T, Zhao J, Xu K, Xu Q (1997) Study on the tribological properties of ultradispersed diamond containing soot as an oil additive. *Tribol Trans* 40:178–182
21. Lakshmi R-V, Bharathidasan T, Basu B-J (2011) Superhydrophobic sol-gel nanocomposite coatings with enhanced hardness. *Appl Surf Sci* 257:10421–10426